

## Photoluminescence studies of amorphous and thermal-aged poly(*p*-phenylene sulfide) films

Zhengda Pan\* and James P. Wicksted

*Department of Physics, Center for Laser Research, Oklahoma State University, Stillwater, Oklahoma 74078*

Huimin Liu

*Department of Physics, University of Puerto Rico at Mayaguez, Mayaguez, Puerto Rico 00681*

(Received 2 December 1992)

Photoluminescence studies have been carried out on several amorphous poly(*p*-phenylene sulfide) (PPS) films using a frequency-tripled pulsed Nd:yttrium aluminum garnet laser at 355-nm wavelength. The main luminescence is attributed to the  $\pi^* \rightarrow \pi$  transition where  $\pi^*$  represents the first excited singlet state of the PPS molecule. The emission features of the amorphous films with different thermal-aging treatments have been obtained, which revealed that the luminescence intensity was reduced and the peak position was slightly shifted after thermal aging. The luminescence lifetime of PPS has been determined to be 2–4 ns by use of a deconvolution method. In addition, a vibronic structure was observed in the photoluminescence spectra at low temperature with the energy spacing nearly equal to the energy corresponding to the phenylene-sulfur stretching vibration. These low-temperature data were analyzed using the lattice-relaxation model with a two-level system. The results indicate that the Huang-Rhys parameter and the temporary lattice distortion slightly decrease with the thermal aging of the polymer.

### I. INTRODUCTION

Poly(*p*-phenylene sulfide) (PPS) is a semicrystalline thermoplastic polymer which possesses excellent mechanical, electrical, thermal, and chemical resistance properties. Enhancement of these properties of PPS have been obtained through thermal-aging treatment for a variety of products and applications.<sup>1</sup> PPS is also a nonrigid, not-fully-carbon-backbone-linked polymer made conducting by AsF<sub>5</sub> doping.<sup>2–5</sup> The pristine polymer is commercially available. It is easily melt processible, an important property for potentially obtaining commercially viable conduction plastics. PPS therefore has attracted considerable interest in order to understand its structural, electrical, and electronic properties. Many different experiments have been devoted to the studies of both pristine and doped PPS in the last decade,<sup>6–11</sup> including absorption<sup>12</sup> and chemiluminescence.<sup>13</sup> However, because of its chemical complexity and the lack of an attractive physical model such as the soliton, the research on the electronic properties of PPS still lags behind that of conjugated polymers. Questions concerning the spectral and temporal behavior of PPS emission still remain. Little data on PPS photoluminescence (PL) have been reported.<sup>13</sup>

In this paper we present the photoluminescence spectra from a set of amorphous PPS films with different thermal-aging treatments, excited at 355 nm by a pulsed Nd:YAG. The main luminescence of PPS is attributed to the  $\pi^* \rightarrow \pi$  transition.<sup>14</sup>  $\pi^*$  represents the first excited singlet state of the PPS molecule which may possibly be described as an exciton state.<sup>15</sup> We found that the PL intensity and shape are dependent on the duration of the thermal-aging treatment. We used a deconvolution method to determine the luminescence decay which is approximately exponential with a lifetime independent of the thermal-aging treatment. We also discuss the tem-

perature dependence of PL from PPS films. We observed a vibronic structure in the PL spectra at low temperatures, which indicates that the transition of the  $\pi$  electron is coupled to the intrachain stretching vibration. A lattice-relaxation model with a two-level system was then developed to interpret the experimental data. Our results show that the electron-lattice coupling strength in PPS is slightly reduced after the thermal-aging treatment.

### II. EXPERIMENT

The samples used for this study were obtained from Phillips Petroleum Company. Amorphous films with and without thermal-aging treatments were supplied. The thicknesses of films were about 65  $\mu\text{m}$ . These films were fabricated by a heat compression molding technique whereby the material is pressed between two steel plates at 500–600 psi at a temperature of 320 °C. After molding, the amorphous films are quickly transferred to a cold press, thus rapidly quenching the material. The average molecular weight of these polymer films is between 40 000 and 50 000.<sup>7</sup> In the thermal-aging process the polymer powder is heated to 260 °C in air for a specified number of hours succeeded by a fast cooling (2–3 min). PPS has a crystalline melting point  $T_m$  of 285 °C and a glass transition temperature  $T_g$  of 85 °C, respectively.<sup>1</sup> The trimer and tetramer samples used in absorption measurements were in the CCl<sub>4</sub> solution. The formulas of trimer and tetramer are (C<sub>6</sub>H<sub>5</sub>-S-C<sub>6</sub>H<sub>4</sub>-S-C<sub>6</sub>H<sub>5</sub>) and (C<sub>6</sub>H<sub>5</sub>-S-C<sub>6</sub>H<sub>4</sub>-S-C<sub>6</sub>H<sub>4</sub>-S-C<sub>6</sub>H<sub>5</sub>), respectively.

The experimental system used for PL measurements is shown in Fig. 1. The excitation source was a Spectra Physics GCR-4 Nd:YAG laser, using its third harmonic at 355 nm with a pulse width of 6 ns, operating at 10 Hz. The energy of the laser beam was reduced to about 50  $\mu\text{J}$  per pulse. The light was incident on the PPS sample at an angle of about 45°. The light emitted from the sample

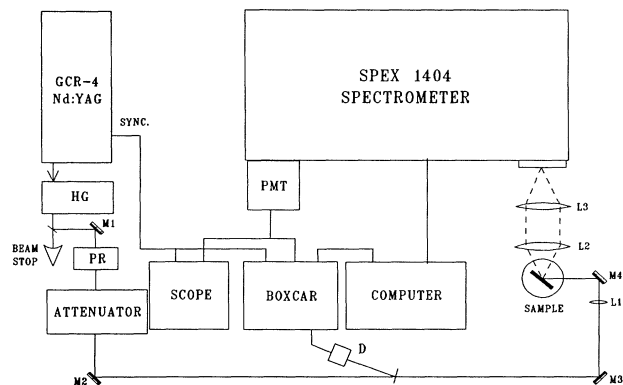


FIG. 1. Experimental setup for photoluminescence measurements.

was collected at a right angle to the incident beam, focused onto the entrance slits of a SPEX 1404 double grating spectrometer and detected by a HAMAMATSU R943-02 photomultiplier tube (PMT) which was cooled to  $-25^{\circ}\text{C}$ . The signal from the PMT was directed into an EG&G 4422 gated sampler with impedance of  $50\Omega$  and averaged by the 4420 Boxcar Averager. For fast lifetime measurements the appropriate impedance match between the electronics and BNC cable connection was carefully determined in order to avoid introducing signal distortion. The spectral response of our experimental system from 360 to 660 nm has been calibrated by using a standard quartz tungsten halogen (QTH) lamp from the Eppley Laboratory. This allowed all of our PL spectra to be corrected. The absorption spectra were measured using a Cary 2400 spectrophotometer.

### III. RESULTS

#### A. Absorption spectra

The absorption spectra of the unaged PPS film, as well as its trimer and tetramer oligomers in  $\text{CCl}_4$  solution, were measured at room temperature in the region from 300 to 400 nm. As shown in Fig. 2, the absorption edge significantly shifts to longer wavelengths when the phenylene-sulfide chain is extended from trimer (3-phenyl rings), to tetramer (4-phenyl rings), to polymer ( $\sim 400$ -phenyl rings). The absorption edges (at an absorbance value of 2.0) are at 328, 338, and 364 nm, corresponding to the trimer, tetramer, and amorphous PPS film, respectively. The energy gap decreases when the  $\pi$ -orbital overlap extends over more phenylene rings. This property indicates that even though the phenyl rings are orthogonal to one another, the appreciable delocalization of the  $\pi$  electrons along the PPS chain still exists. This result is in agreement with the previous study by Bredas *et al.*<sup>16</sup>

Figure 3 shows the absorption spectra from a set of amorphous PPS films with different durations of the thermal-aging treatments. The spectrum of aged samples has a higher absorption tail and shows higher broadband absorption in the visible region compared with that of the unaged sample. The absorption edges represent the

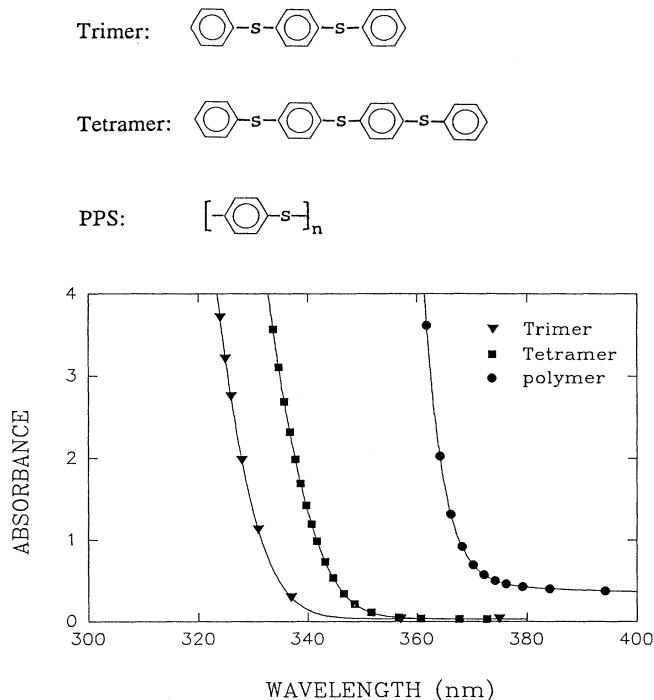


FIG. 2. Room-temperature absorption spectra from an unaged amorphous PPS film, and from the trimer and tetramer oligomers in the  $\text{CCl}_4$  solution.

$\pi \rightarrow \pi^*$  transition in PPS.<sup>14</sup> The sharp absorption edge shifts from 364 nm for the unaged film to 365.5 for the 2-h aged sample and shifts slightly further for samples with longer aging time. The absorption peak was taken at 326 nm for the unaged PPS film from the absorption spectrum of a PPS thin film reported by Friend and Giles.<sup>12</sup> It has been reported<sup>7</sup> that cross linking, chain extension, and oxidization may occur when PPS is thermal aged in air at  $260^{\circ}\text{C}$ . Therefore, the higher absorption tail reflects the collective absorption behavior from the thermal degraded PPS molecules. The broadband absorptions in the visible region are from chemical species which have smaller energy gaps. These more colored species were

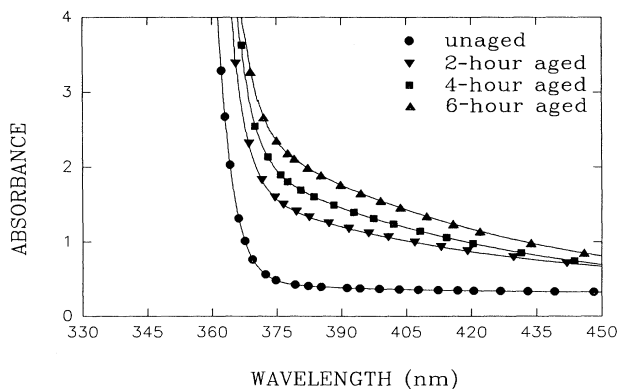
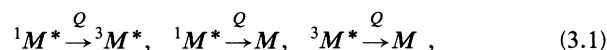


FIG. 3. Room-temperature absorption spectra from a set of amorphous PPS films with different aging times.

formed during heating of the polymer in air. These species possibly possess double bonds between carbon and sulfur atoms.<sup>17</sup>

### B. Room-temperature photoluminescence

The PL spectra shown in Fig. 4 were from a set of amorphous PPS films with different durations of the thermal-aging treatments. All these PL spectra show a broadband emission with the maximum around 380 nm. The FWHM (full width at half maximum) for each sample is about  $2600\text{ cm}^{-1}$ . This broadband feature is due to the amorphous nature of the film and the multiphonon-assisted transitions.<sup>18</sup> The main peak of the luminescence is attributed to the  $\pi^* \rightarrow \pi$  singlet transition. The  $\pi$  electron in PPS is partially delocalized along the chain.<sup>19</sup> As a result, the dominant electronic excitations are inherently coupled to the chain distortions. The intensity of the fluorescence from aged films is reduced while the broad band emission at longer wavelengths is relatively enhanced. The reduction in peak intensity from the aged films is probably due to the presence of quenching impurities<sup>20</sup> which were unintentionally introduced during the heating of the PPS in air. This process of impurity quenching is commonly due to an increase in the rate of both intersystem and intrasystem crossing from the first excited singlet state to the first triplet state and to the ground state in the presence of the quencher.<sup>20</sup> The process can be represented as



where  ${}^1M^*$ ,  ${}^3M^*$ , and  $M$  represent first singlet excited state, first triplet state, and the ground state of the PPS molecule while  $Q$  is the quencher. Such quenching behavior is typical of impurities such as oxygen. Previous investigations<sup>7,21</sup> confirmed that the oxygen atoms entered the polymer when PPS was treated close to its melting point in air. In addition, the energy of the excited state of PPS molecules may also be transferred to secondary radiating centers which, in turn, emit their own luminescence in the region of longer wavelengths. These emissions at longer wavelengths are increased for aged samples.

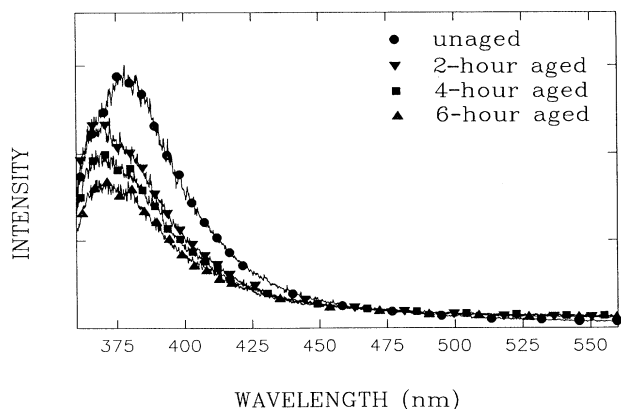


FIG. 4. Room-temperature PL spectra from a set of amorphous PPS films with different aging times.

We also noticed that the peak position of the PL from the aged PPS films was slightly shifted to shorter wavelengths, while the absorption edge was shifted to longer wavelengths. Presumably, this is due to the change of the electron-vibration coupling strength after the aging processing. We will discuss the electronic-vibration coupling in PPS in a later section.

### C. Emission decay of PPS

The fluorescence lifetime measurements were carried out using a deconvolution technique owing to the comparable events in the time range between the PL decay and the light source duration of 6 ns. In addition, the PMT rise time is also of concern. At room temperature, we measured the temporal decay profiles of all PPS films at their peak positions (380–385 nm). We found that different samples have almost the same decay profiles. The lifetime was found to be  $2.6 \pm 0.5$  ns at the peak position. At a low temperature of  $T = 6$  K, we measured the emission profiles at both the main peak (365–370 nm) and the second peak (380–385 nm). We found that the luminescence at these two peaks has exactly the same decay profiles. The fluorescence lifetime is  $3.2 \pm 0.5$  ns. Although each lifetime value obtained has a significant error bar, they are still valuable because no fluorescence

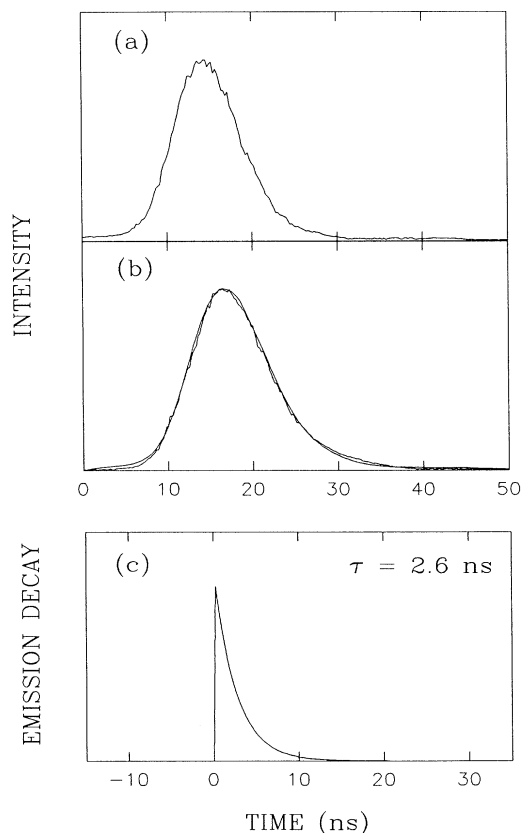


FIG. 5. Deconvolution of the laser pulse and the emission pulse for an amorphous PPS film at room temperature. (a) The measured laser pulse, (b) the measured emission pulse, (c) the deconvoluted emission decay result.

lifetime data of PPS have been available in the literature.

The situation at room temperature is illustrated in Fig. 5, where  $\tau=2.6$  ns gives the best fit; the situation at  $T=6$  K is illustrated in Fig. 6 where  $\tau=3.2$  ns. In both cases the exponential decay fits are consistent with the measured results. This indicates that the actual emission decay is approximately exponential.

#### D. Low-temperature photoluminescence

The PL spectra at temperatures of 293, 150, 80, and 6 K from an amorphous PPS film are shown in Fig. 7. The PL intensity increases when temperature decreases. At low temperatures the emission spectrum shows two well-resolved peaks at 367 and 382 nm. The low-energy emission with a long tail extending to about 500 nm can be recognized as phonon sidebands associated with the vibrational states of the polymer chain. The energy spacing between the two peaks is about  $1080\text{ cm}^{-1}$ , which is similar to the energy of the intrachain phenylene-sulfur stretching vibration. The latter has an energy of  $1076\text{ cm}^{-1}$  as determined from our Raman measurements.<sup>22</sup>

Figure 8 shows PL spectra at temperatures of 293, 150, 80, and 6 K from a 2-h aged amorphous PPS film. The fabrication of this sample is the same as the amorphous film except for the thermal-aging treatment. The main

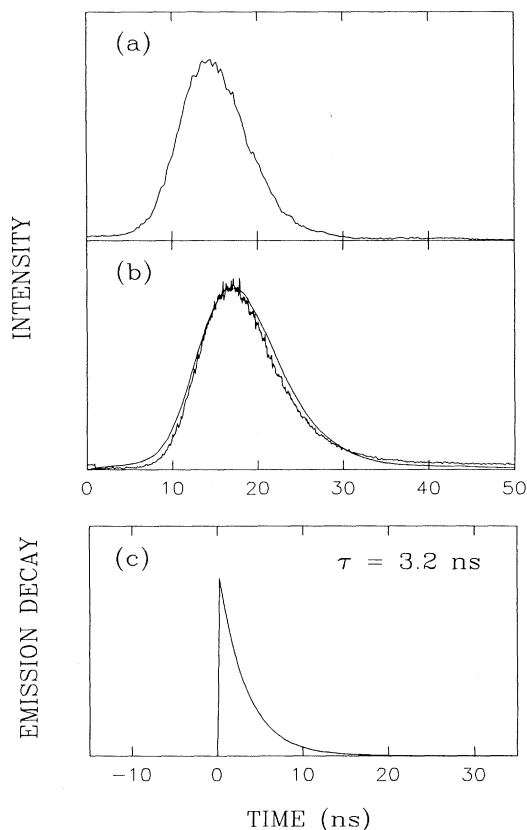


FIG. 6. Deconvolution of the laser pulse and the emission pulse for an amorphous PPS film at  $T=6$  K. (a) The measured laser pulse, (b) the measured emission pulse, (c) the deconvoluted emission decay result.

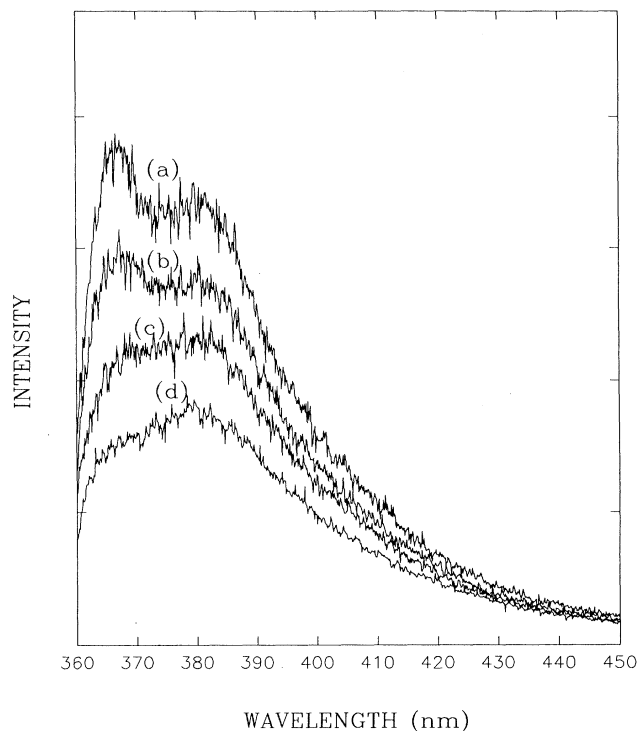


FIG. 7. PL spectra of an unaged amorphous PPS film at four different temperatures: (a)  $T=6$  K, (b)  $T=80$  K, (c)  $T=150$  K, (d)  $T=293$  K.

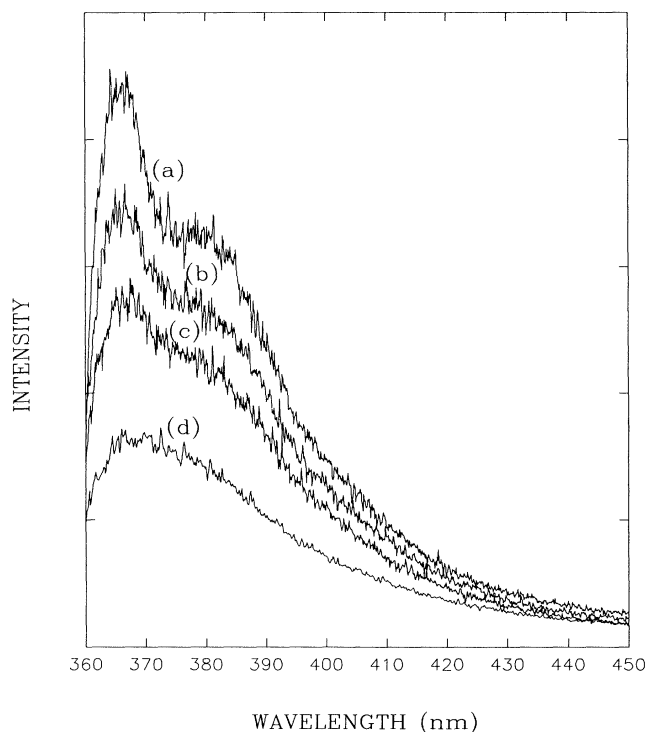


FIG. 8. PL spectrum of a 2-h aged amorphous PPS film at four different temperatures: (a)  $T=6$  K, (b)  $T=80$  K, (c)  $T=150$  K, (d)  $T=293$  K.

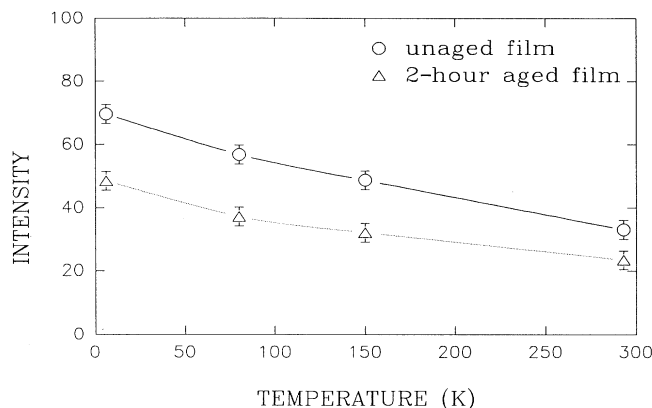


FIG. 9. Temperature dependence of the PL peak intensities for the amorphous and 2-h aged films.

peak and the sideband of the low-temperature spectrum are at 366 and 381 nm, respectively. Note that the energy difference between these two peaks once again corresponds to the energy of the intrachain phenylene-sulfur stretching mode. Comparing the spectra of the aged film with that of the unaged film, it is found that the relative intensity between the main peak and sideband is changed significantly. The main peak of PL is much more intense than the sideband from the aged film. The peak position in the PL spectrum of the aged sample is shifted towards higher energy by about  $80 \text{ cm}^{-1}$  ( $\Delta\lambda \approx 1.1 \text{ nm}$ ), while the absorption is shifted towards lower energy by about  $120 \text{ cm}^{-1}$  ( $\Delta\lambda \approx 1.5 \text{ nm}$ ) (see Fig. 3).

The temperature dependences of the PL peak intensities from an amorphous film and a 2-h aged amorphous film are shown in Fig. 9. The peak intensity of PL decreases when temperature increases. This is reasonable because at high temperature the quenching rate is increased for organic materials.<sup>23</sup>

#### IV. INTERPRETATION OF THE EXPERIMENTAL RESULTS

The experimental results described above show that the  $\pi^* \rightarrow \pi$  transitions in PPS are coupled predominantly to the phenylene-sulfur stretching vibration along the PPS backbone.<sup>22</sup> The  $\pi \rightarrow \pi^*$  excitation causes the temporary lattice deviation owing to the lattice relaxation.<sup>24–27</sup> The strength of the electron-lattice coupling of an electronic state depends strongly upon the spatial extent of that state. The spectral changes of PPS films upon aging seem related to the change in the electron-lattice coupling strength. Based on the above information we used the lattice-relaxation theory<sup>24,25</sup> to interpret the experimental results.

##### A. Physical model for vibronic transitions

In general, there are interactions between the  $\pi$  electrons of the phenylene rings and their neighboring atoms in a PPS molecule. The electronic transition of the localized  $\pi$  electron changes the equilibrium position of the surrounding sulfur atoms in the polymer lattice. To sim-

plify, we take the phenylene ring with its  $\pi$ -electron system as a single unit. The center of the ring represents the average nuclear position in the lattice. The  $\pi$  electron in a phenylene ring interacts with its surroundings, behaving as the electron-lattice interaction. The total Hamiltonian of the electron-lattice interaction system can be written as

$$H = H_e + H_{eL} + H_L, \quad (4.1)$$

where  $H_e$ ,  $H_{eL}$ , and  $H_L$  represent the electronic, electron-phonon, and lattice vibration Hamiltonians, respectively. In the adiabatic approximation, the total wave function of the system can be written as a product of two functions:

$$\Psi_i(r, q) = \phi_i(r, q) \chi_{i,n}(q), \quad (4.2)$$

where  $r$  represents the electronic coordinates and  $q$  represents the nuclear coordinates; the function  $\phi_i(r, q)$  is an electronic wave function which depends parametrically on the nuclear coordinates and  $\chi_{i,n}(q)$  is a vibrational wave function which describes the nuclear motion. The electronic and vibrational wave functions are solutions of the following eigenvalue equations.<sup>24</sup>

$$(H_e + H_{eL})\phi_i(r, q) = E_i(q)\phi_i(r, q), \quad (4.3)$$

$$(H_L + E_i(q))\chi_{i,n}(q) = E_{i,n}\chi_{i,n}(q). \quad (4.4)$$

The first equation of the system describes the stationary states of the electrons in the adiabatic approximation. The second equation of the system describes the motion of nuclei in the molecule and is denoted as the vibrational equation.

In a simplified model, the electron-phonon interaction Hamiltonian  $H_{eL}$  and the electronic eigenvalue  $E_i(q)$  are taken as linear functions of the lattice coordinates  $q_k$ . The influence of localized electronic states on the lattice vibration results in the displacement of the lattice equilibrium position.<sup>25</sup>

In the following, two levels,  $i$  and  $j$ , of the system are assumed. For an optical transition (emission or absorption), the transition probability is proportional to the square of the transition matrix element. For localized centers showing lattice relaxation, the atomic configuration changes with the transition, so in forming the transition matrix element, the atomic vibrational wave functions  $\chi_{i,n}(q)$ ,  $\chi_{j,n'}(q)$ , as well as the electronic wave functions  $\phi_i(r)$  and  $\phi_j(r)$  have to be taken into account. So one should write the transition probability

$$W_{\text{rad}} \propto \left| \int \chi_{j,n'}(q) \left[ \int \phi_j er \phi_i dr \right] \chi_{i,n}(q) dq \right|^2, \quad (4.5)$$

where the electric dipole moment  $er$  is assumed. As the integral over the electronic coordinates can be considered as approximately independent of the vibrational coordinates (the ‘‘Condon approximation’’), one has approximately

$$\int \phi_i(r, q) er \phi_j(r, q) dr = M_{ij}, \quad (4.6)$$

which is independent of lattice coordinates  $q$ . The optical transition probability then is approximately

$$W_{ij} \propto M_{ij}^2 \left| \int \chi_{j,n}(q) \chi_{i,n}(q) dq \right|^2. \quad (4.7)$$

In this formula, the vibronic transition probability is determined by the overlap integral between the initial- and final-state vibrational wave functions.

Based on Eq. (4.7) we can predict that if a single phonon mode of frequency  $\omega_0$  is involved, the emission spectrum will include a series of lines with frequencies

$$E = E_{j \rightarrow i} - p \hbar \omega_0. \quad (4.8)$$

This kind of spectral structure is known as the vibronic structure and  $p$  is an integer.

Usually, a single-mode approximation is used to analyze the multiphonon vibronic structure in a spectrum. For a polymer system, a two-level configuration coordinate model is a good approximation<sup>28</sup> to account for the lattice relaxation (Fig. 10). The main peak in the absorption spectrum corresponds to a vertical transition from the vibronic ground state of the level  $i$  to the vibronic state of the level  $f$  ( $A \rightarrow B$ ) while the main peak in the emission spectrum corresponds to a vertical transition from the vibronic ground state of the level  $f$  to the vibronic state of  $i$  ( $C \rightarrow D$ ). Using the harmonic approximation, the Stokes loss, which is the energy spacing between the main absorption peak and the zero-phonon emission line, is

$$L = \frac{1}{2} \omega^2 \Delta_{if}^2, \quad (4.9)$$

where  $\Delta_{if}$  is the displacement of the two adiabatic potential curves in the normalized configurational coordinate. We can write the Stokes loss in terms of the number of vibrational quanta which is

$$S = \frac{L}{\hbar \omega} = \frac{\omega}{2\hbar} \Delta_{if}^2. \quad (4.10)$$

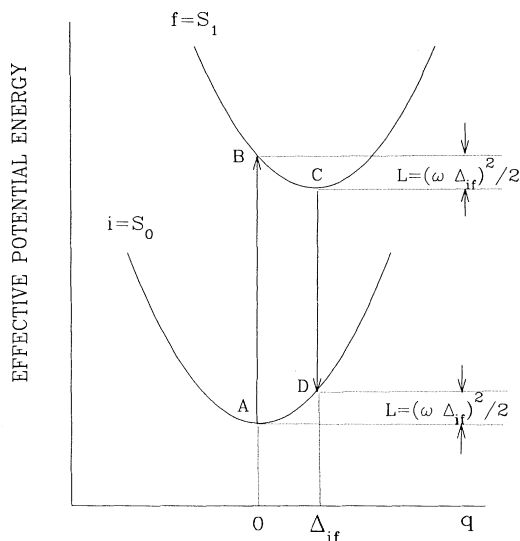


FIG. 10. Configurational coordinate diagram for two levels  $i$  and  $f$ . The lower parabola represents the potential curve of the ground electronic state of the PPS molecule while the upper parabola represents the potential curve of the excited electronic state. The abscissa  $q$  represents the configurational coordinate.

Here,  $S$  is known as the Huang-Rhys parameter<sup>29</sup> describing the strength of the electron-phonon coupling. The Huang-Rhys parameter  $S$  can also be used in a general situation with multiple vibrational modes and is written as<sup>25</sup>

$$S = \sum_k \left[ \frac{\omega_k}{2\hbar} \right] \Delta_{if,k}^2. \quad (4.11)$$

The Stokes loss then becomes

$$L = S \langle \hbar \omega \rangle_{av} = S \hbar \omega_{eff}, \quad (4.12)$$

where the weighted average is over all phonon modes and  $\omega_{eff}$  is the effective phonon frequency.

Now consider the vibronic transition from the zero vibronic state of the upper level  $\phi_{1,0}$  to the vibronic state of the lower level  $\phi_{0,n}$ , corresponding to the transition at the low-temperature limit. Using harmonic-oscillator eigenfunctions, the overlap integral between the initial- and final-state vibrational wave functions can be solved:<sup>30</sup>

$$\left| \int \chi_{10}(q) \chi_{0n}(q) dq \right|^2 = e^{-s} \frac{S^n}{n!}. \quad (4.13)$$

The distribution of the emission intensity versus energy then can be written as

$$I = M_{fi} e^{-s} \left[ \frac{S^n}{n!} \right]. \quad (4.14)$$

This formula is known as the ‘‘Pekar Formula’’ which follows a Poisson distribution.  $M_{fi}$  is the matrix element of the transition between the excited and ground electronic states,  $S$  is the Huang-Rhys parameter, and value  $e^{-s}$  is the Condon factor, giving the relative size of the transition which occurs without the creation or annihilation of phonons ( $0 \rightarrow 0$  line), and  $n = 0, 1, 2, \dots$ , which represents the number of phonons involved in a transition.

In our PL measurements, the excited source used is at a wavelength of 355 nm which excites only the first  $\pi^*$  singlet state of the PPS molecule. Therefore, we can use a two-level system to analyze the localized  $\pi$ -electronic system of the poly(*p*-phenylene sulfide) film: a ground level and an excited level. The dominant vibrational mode which couples to the  $\pi^* \rightarrow \pi$  transition will be shown to be the phenylene-sulfur stretching mode.

### B. The electron-lattice coupling in PPS

Based on the physical model described above, the main PL peak is associated with the vertical transition from the zero vibronic state of the upper level to the vibronic state of the lower level ( $C \rightarrow D$  in Fig. 10); the main PL peak of the unaged amorphous PPS film is at about  $27\,250 \text{ cm}^{-1}$  (367 nm). The absorption peak is associated with the vertical transition from the zero vibronic state of the lower level to the vibronic state of the upper level ( $A \rightarrow B$  in Fig. 10). The absorption peak was taken at  $30\,680 \text{ cm}^{-1}$  (326 nm).<sup>12</sup> The Stokes shift is then about  $1700 \text{ cm}^{-1}$ . The  $1076\text{-cm}^{-1}$  phonon appears to dominate the spacing between the peaks in the low-temperature PL spectrum (Fig. 7). Therefore, it was used as the effective

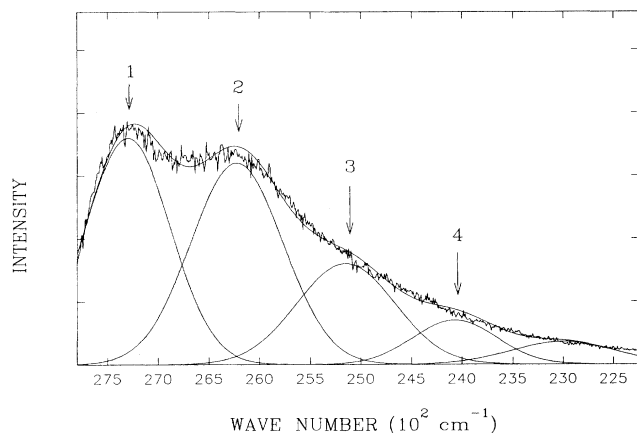


FIG. 11. Curve fitting for PL spectrum of an unaged amorphous PPS film at  $T=6$  K. The decomposed vibronic structure shows different phonon orders with Gaussian-shaped lines.

frequency in Eq. (4.12) allowing the Huang-Rhys parameter  $S \approx 1.6$  for the unaged amorphous PPS film to be determined. This value is larger than the  $S$  value of 1.1 in poly(3-methylthiophene) reported by Poplawski and Ehrenfreund.<sup>31</sup> This result indicates that the electron-lattice coupling in PPS is greater than that in poly(3-methylthiophene). It indicates that the  $\pi$  electron in PPS is less extended than the  $\pi$  electron in this latter conjugated polymer.

Figure 11 shows the analysis for the PL spectrum of an unaged amorphous PPS film at 6 K. Based on the "Pekar formula" (4.14), the PL spectrum is composed of a main peak and the accompanied sidebands with a neighboring energy spacing of  $1076 \text{ cm}^{-1}$ . We used a curve fitting program to fit the PL spectrum by adding a series of Gaussian-shape lines with spacing of  $1076 \text{ cm}^{-1}$ . Each subsequent band corresponds to different phonon orders (Table I). The relative intensities of these bands approximately follow the Poisson distribution with  $S=1.6$ . The intensity ratio between the first and second peaks is about 1.2. The mechanism of the large bandwidth is mainly attributed to the inhomogeneous broadening. The polymer sample is a complicated molecular ensemble and has an amorphous nature. The molecules in a polymer sample have different molecular weights which are widely distributed between 40 000 and 50 000.<sup>7</sup> There are derivants, faults, unintentional impur-

TABLE I. The curve fitting results of the PL spectrum from an unaged PPS film (see Fig. 11).

Phonon orders			
1	2	3	4
Peak positions ( $\text{cm}^{-1}$ )			
27 250	26 170	25 094	24 018
Standard deviations ( $\text{cm}^{-1}$ )			
418	455	483	412

ities, etc., inside the sample. The frequency of a transition is influenced by the molecular change as well as environmental change. Hence, the profile, being a composite of the transitions from different sites, shows a Gaussian line shape.

Figure 12 illustrates the analysis for the PL spectrum of a 2-h aged PPS film at 6 K. The spectrum is composed of a main peak and sidebands with the same energy spacing of  $1076 \text{ cm}^{-1}$  as in the spectrum of an unaged sample. The Stokes shift for the aged PPS sample is reduced because its absorption spectrum is shifted to a longer wavelength while its emission spectrum is shifted to a shorter wavelength. The Stokes shift for the 2-h aged PPS film is reduced to about  $1600 \text{ cm}^{-1}$  and a value of  $S \approx 1.5$  was obtained. The change of the  $S$  value indicates that the strength of electron-phonon coupling in PPS is modified after the aging process. According to the Poisson distribution (4.14), the change of the  $S$  value will modify the relative intensity among the main peak and sidebands in a PL spectrum. This has been seen in Fig. 12 where the spectrum shows a distinct intensity ratio of the main peak emission to the sideband. The intensity ratio between first and second peaks for an aged sample is 1.36, which approximately follows the Poisson distribution. The reduced Stokes shift for an aged PPS film also implies that the displacement  $\Delta_{if}$  of the configurational coordinate between two electronic levels in the aged sample is a little smaller than that in the unaged PPS film. The results of the curve fitting for PL spectra (Figs. 11 and 12) from an unaged and a 2-h aged PPS films are listed in Tables I and II, showing the peak positions and standard deviations for different phonon orders.

We can relate the Stokes shift  $Sh\omega$  to the lattice distortion energy and solve the lattice distortion  $\Delta'_{if}$  upon knowing the lattice force constant. Using the data obtained in a previous paper,<sup>22</sup> the effective force constant for the phenylene-sulfur displacement is  $C_{\text{eff}} \approx 16$  (mdyn/Å). We can estimate the lattice distortion  $\Delta'_{if}$  in terms of

$$\Delta'_{if} = \frac{\Delta_{if}}{\sqrt{\mu}}, \quad (4.15)$$

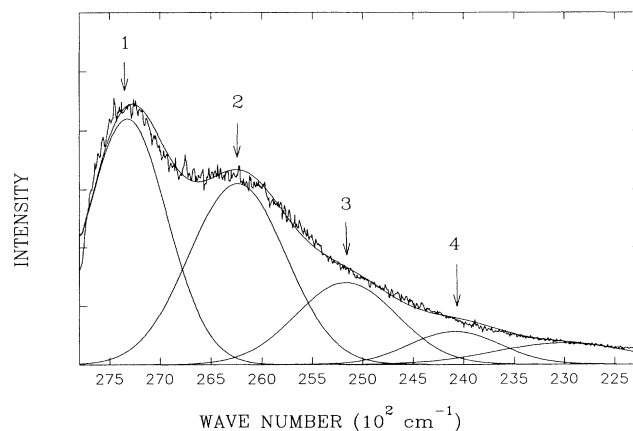


FIG. 12. Curve fitting for PL spectrum of a 2-h aged amorphous PPS film at  $T=6$  K. The decomposed vibronic structure shows different phonon orders with Gaussian-shaped lines.

TABLE II. The curve fitting results of the PL spectrum from a 2-h aged PPS film (see Fig. 12).

Phonon orders			
1	2	3	4
Peak positions (cm <sup>-1</sup> )			
27 330	26 250	25 174	24 098
Standard deviations (cm <sup>-1</sup> )			
397	474	499	447

where  $\mu$  is the effective mass and  $\Delta'_{if}$  has the unit of length. The lattice distortion energy,  $\frac{1}{2}C_{\text{eff}}(\Delta'_{if})^2$ , is equal to the Stokes shift in our model. We then solved the lattice distortion  $\Delta'_{if} \approx 0.065 \text{ \AA}$  for the unaged amorphous PPS film and  $\Delta'_{if} \approx 0.062 \text{ \AA}$  for the 2-h aged film. The distance between the center of phenylene ring and sulfur atom is  $3.13 \text{ \AA}$ , which was obtained from the lattice size of PPS given by Tabor, Magre, and Boon.<sup>32</sup> The distortion therefore is about 2.1%. The lattice-relaxation parameters for an unaged amorphous PPS film and a 2-h aged PPS film are listed in Table III.

In general, the strength of the electron-lattice coupling of an electronic state depends strongly upon the spatial extent of that state.<sup>33</sup> When the state is confined to a single atomic site, the strength of the coupling of the electronic state to the lattice is large, much greater than 1; whereas, when the state extends over many sites, the electron-lattice interaction is, in general, much smaller. Because the electronic state only interacts effectively with atomic vibrations having wavelengths greater than its characteristic length, a short-range electron-lattice interaction, such as the deformation potential, will have a coupling strength varying inversely to the spatial extension of the state. Thus, an electronic state which is confined to an atomic site will have a large value of the coupling strength  $S$  whereas a state which extends over a large monomer will have a small- $S$  value (i.e., coupling to the lattice vibrations would be weak). These differences are of crucial importance in discussing the magnitude and temperature dependence of the hopping conductivity among such states.<sup>33</sup> As indicated by our absorption results as well as previous studies,<sup>16,19</sup> the  $\pi$  electron in PPS is partially delocalized along the chain; therefore, we expect to have a smaller- $S$  value. Previous investigations also indicated that both interchain and intrachain crosslinking in PPS occurred during the aging processing<sup>34</sup> and the photoconductivity near the absorption edge was significantly enhanced after PPS was annealed in oxygen at temperatures ranging from 250 to 295°C.<sup>35</sup> The intrachain crosslinking will increase the  $\pi$ -orbital overlap along the PPS chain. The increased photoconductivity is the evidence of this behavior. Therefore, the electron-lattice coupling strength should be reduced for aged samples, which is consistent with our PL results.

TABLE III. The electron-phonon coupling parameters.

No.	$L^c$ (cm <sup>-1</sup> )	$E_1^d$ (cm <sup>-1</sup> )	$E_2^e$ (cm <sup>-1</sup> )	$E_1 - E_2$	$S$	$\Delta'_{if}$ (\AA)
1 <sup>a</sup>	1 700	27 250	26 170	1 080	1.6	0.065
2 <sup>b</sup>	1 600	27 330	26 250	1 080	1.5	0.062

<sup>a</sup>An unaged amorphous film.

<sup>b</sup>A 2-h aged film.

<sup>c</sup>Stokes shift.

<sup>d</sup>Main peak.

<sup>e</sup>Sideband.

## V. SUMMARY

The absorption and PL spectra from various amorphous PPS films with different thermal treatment were reported. The excitation of the  $\pi$  electron in PPS may form a localized electron-hole pair and the PL of PPS could be attributed to these intrachain excitons. The  $\pi$ -electron system plays a key role in determining the electronic properties of PPS, such as the conductivity upon doping. Previous studies indicated that the  $\pi$  electron in PPS is partially delocalized along the chain. As a result, the dominant electronic excitations are inherently coupled to chain distortions. Our low-temperature measurements show that the photoluminescence of PPS films is accompanied by strong phonon sidebands whose frequency is similar to the phenylene-sulfur stretching vibrations in the polymer backbone. The lattice-relaxation model with a two-level system was then used to analyze the PL data. The lower level represents the ground electronic state and the upper level represents the excited state ( $\pi^*$ ) of the PPS molecule. Our low-temperature PL data were well interpreted by using this model. The electron-phonon coupling strength, the Huang-Rhys parameter  $S$ , as well as the temporary lattice distortion  $\Delta'_{i,f}$  between the phenylene ring and sulfur atom were determined for both the unaged amorphous PPS film and the 2-h aged PPS film. The results show that the strength of the electron-lattice coupling was slightly changed after the aging process. This change is expected because the  $\pi$ -orbital overlap along the PPS chain was increased after the aging process. In addition, the luminescence decay lifetime was determined by using a deconvolution method. The room-temperature PL intensity and peak shape, which are related to the sample morphology and the thermal process, were also discussed.

## ACKNOWLEDGMENTS

We would like to acknowledge F. Wood-Black, M. Dreiling, and P. K. Das of Phillips Petroleum Company for providing all the PPS films used in this study. Support for this work was provided by the Oklahoma Center for the Advancement of Science and Technology (OCAST) under Contract No. 3757.

- \*Present address: Department of Physics, Fisk University, Nashville, TN 37208.
- <sup>1</sup>J. F. Geibel and R. W. Campell, in *Comprehensive Polymer Science*, edited by G. C. Eastmond (Pergamon, New York, 1989), Vol. 5, p. 543.
- <sup>2</sup>J. F. Rabolt, T. C. Clarke, K. K. Kanazawa, J. R. Reynolds, and G. B. Street, *J. Chem. Soc. Chem. Commun.* **8**, 347 (1980).
- <sup>3</sup>R. R. Change, L. W. Shacklette, G. G. Miller, D. M. Ivory, R. L. Elsenbaumer, and R. H. Baughman, *J. Chem. Soc. Chem. Commun.* **8**, 348 (1980).
- <sup>4</sup>L. W. Shacklette, R. L. Elsenbaumer, R. R. Chance, H. Eckhardt, J. E. Frommer, and R. H. Baughman, *J. Chem. Phys.* **75**, 1919 (1981).
- <sup>5</sup>R. L. Elsenbaumer and L. W. Shacklette, in *Handbook of Conducting Polymers*, edited by T. A. Skotheim (Dekker, New York, 1986), p. 213.
- <sup>6</sup>J. P. Buisson, J. Y. Mevellec, S. Zeraoui, and S. Lefrant, *Synth. Met.* **41-43**, 287 (1991).
- <sup>7</sup>C.-H. M. Ma, L.-T. Hsiue, W.-G. Wu, and W.-L. Liu, *J. Appl. Polym. Sci.* **39**, 1399 (1990).
- <sup>8</sup>K. C. Cole, D. Noel, and J. J. Hechler, *J. Appl. Polym. Sci.* **39**, 1887 (1991).
- <sup>9</sup>Y. Tanabe, H. Shimizu, and N. Minami, *Jpn. J. Appl. Phys.* **27**, 1748 (1988).
- <sup>10</sup>A. J. Lovinger, F. J. Padden, Jr., and D. D. Davis, *Polymer* **29**, 229 (1988).
- <sup>11</sup>S. Asada, K. Seki, and H. Inokuchi, *Chem. Phys. Lett.* **130**, 155 (1986).
- <sup>12</sup>R. H. Friend and J. R. M. Giles, *J. Chem. Soc. Chem. Commun.* **16**, 1101 (1984).
- <sup>13</sup>S. K. Brauman, *J. Polym. Sci. A* **27**, 3285 (1989).
- <sup>14</sup>M. D. Lumb, *Luminescence Spectroscopy* (Academic, New York, 1978), p. 95.
- <sup>15</sup>R. H. Fried, D. D. C. Bradley, and P. D. Townsend, *J. Phys. D* **20**, 1367 (1987).
- <sup>16</sup>J. L. Bredas, R. L. Elsenbaumer, R. R. Chance, and R. Silbey, *J. Chem. Phys.* **78**, 5656 (1983).
- <sup>17</sup>W. T. Ford (private communication).
- <sup>18</sup>K. Huang, *Contemp. Phys.* **22**, 599 (1981).
- <sup>19</sup>G. Grecelius, J. Fink, J. J. Ritsko, M. Stamm, H.-J. Freund, and H. Gonska, *Phys. Rev. B* **28**, 1802 (1983).
- <sup>20</sup>A. H. Alwattar, M. D. Lumb, and J. B. Birks, in *Organic Molecular Photophysics*, edited by J. B. Birks (Wiley, New York, 1973), p. 414.
- <sup>21</sup>A. Takimoto, E. Tanaka, and M. Watanabe, *Jpn. J. Appl. Phys.* **28**, 1252 (1989).
- <sup>22</sup>Z. Pan, T. Savard, and J. P. Wicksted, *J. Raman Spectrosc.* **23**, 615 (1992).
- <sup>23</sup>A. H. Alwattar, M. D. Lumb, and J. B. Birks, in *Organic Molecular Photophysics*, edited by J. B. Birks (Wiley, New York, 1973), Vol. 1, p. 421.
- <sup>24</sup>K. Huang, *Sci. Sin. China* **116**, 27 (1981).
- <sup>25</sup>K. Huang, *Prog. Phys.* **1**, 31 (1981).
- <sup>26</sup>H. Liu and R. C. Powell, *J. Appl. Phys.* **70**, 20 (1991).
- <sup>27</sup>H. Liu, R. C. Powell, and L. A. Boatner, *Phys. Rev. B* **44**, 2461 (1991).
- <sup>28</sup>W. A. Phillips, *J. Low Temp. Phys.* **7**, 351 (1972).
- <sup>29</sup>K. Huang and A. Rhys, *Proc. R. Soc. London, Ser. A* **204**, 406 (1950).
- <sup>30</sup>B. Di Bartolo, *Radiationless Processes* (Plenum, New York, 1980), p. 75.
- <sup>31</sup>J. Poplawski and E. Ehrenfreund, in *Electronic Properties of Conjugated Polymers III*, edited by H. Kuzmany, M. Mehring, and S. Roth (Springer, New York, 1989), p. 86.
- <sup>32</sup>B. J. Tabor, E. P. Magre, and J. Boon, *Eur. Polym. J.* **7**, 1127 (1971).
- <sup>33</sup>D. Emin, in *Handbook of Conducting Polymers*, edited by T. A. Skotheim (Marcel Dekker, New York, 1986), Vol. 2, p. 992.
- <sup>34</sup>A. B. Port and R. H. Still, *Polym. Degradation Stability* **2**, 1 (1980).
- <sup>35</sup>E. Tanaka, A. Takimoto, and M. Watanabe, *J. Appl. Phys.* **67**, 842 (1990).
- <sup>36</sup>Kendall L. Su, *Time-Domain Synthesis of Linear Networks* (Prentice-Hall, Englewood Cliffs, NJ, 1971), p. 40.